

# Cortical Visual Mapping following Ocular Gene Augmentation Therapy for Achromatopsia

Ayelet McKyton,<sup>1</sup> Edward Averbukh,<sup>2</sup> Devora Marks Ohana,<sup>2</sup> Netta Levin,<sup>1\*</sup> and Eyal Banin<sup>2\*</sup>

<sup>1</sup>fMRI Unit, Department of Neurology, Hadassah Medical Organization and Faculty of Medicine, Hebrew University of Jerusalem, Jerusalem 91120, Israel, and <sup>2</sup>Center for Retinal and Macular Degenerations (CRMD), Department of Ophthalmology, Hadassah Medical Organization and Faculty of Medicine, Hebrew University of Jerusalem, Jerusalem 91120, Israel

The ability of the adult human brain to develop function following correction of congenital deafferentation is controversial. Specifically, cases of recovery from congenital visual deficits are rare. *CNGA3*-achromatopsia is a congenital hereditary disease caused by cone-photoreceptor dysfunction, leading to impaired acuity, photoaversion, and complete color blindness. Essentially, these patients have rod-driven vision only, seeing the world in blurry shades of gray. We use the uniqueness of this rare disease, in which the cone-photoreceptors and afferent fibers are preserved but do not function, as a model to study cortical visual plasticity. We had the opportunity to study two *CNGA3*-achromatopsia adults (one female) before and after ocular gene augmentation therapy. Alongside behavioral visual tests, we used novel fMRI-based measurements to assess participants' early visual population receptive-field sizes and color regions. Behaviorally, minor improvements were observed, including reduction in photoaversion, marginal improvement in acuity, and a new ability to detect red color. No improvement was observed in color arrangement tests. Cortically, pretreatment, patients' population-receptive field sizes of early visual areas were untypically large, but were decreased following treatment specifically in the treated eye. We suggest that this demonstrates cortical ability to encode new input, even at adulthood. On the other hand, no activation of color-specific cortical regions was demonstrated in these patients either before or up to 1 year post-treatment. The source of this deficiency might be attributed either to insufficient recovery of cone function at the retinal level or to challenges that the adult cortex faces when computing new cone-derived input to achieve color perception.

**Key words:** achromatopsia; color; plasticity; population-receptive field; vision; visual cortex

## Significance Statement

The possibility that the adult human brain may regain or develop function following correction of congenital deafferentation has fired the imagination of scientists over the years. In the visual domain, cases of recovery from congenital deficits are rare. Gene therapy visual restoration for congenital *CNGA3*-achromatopsia, a disease caused by cone photoreceptor dysfunction, gave us the opportunity to examine cortical function, to the best of our knowledge for the first time, both before and after restorative treatment. While behaviorally only minor improvements were observed post-treatment, fMRI analysis, including size algorithms of population-receptive fields, revealed cortical changes, specifically receptive field size decrease in the treated eyes. This suggests that, at least to some degree, the adult cortex is able to encode new input.

Received Dec. 29, 2020; revised July 7, 2021; accepted July 15, 2021.

Author contributions: A.M. and N.L. designed research; A.M., D.M.O., and N.L. performed research; E.A. and E.B. contributed unpublished reagents/analytic tools; A.M. and D.M.O. analyzed data; A.M., E.A., N.L., and E.B. wrote the paper.

This investigator-driven study was supported by the Yedidut Research Fund (to E.B.). We thank Dr. Matthew Feinsod for his input. We also thank our patients for their commitment and efforts, and our fellow researchers from additional centers in the United States who are taking part in the NCT02935517 study. In addition, we thank Dr. Hamzah Aweidah, Inbar Erdinest, Asala Onallah, Shelly Stika, Einav Nachmani, and Enosh Wilhelm from the CRMD for excellent clinical and technical assistance; and Dr. Yael Backner (fMRI laboratory) and Professor John Barbur (Optics Chair, City University of London) for contributions in editing the article.

The authors declare no competing financial interests.

\*N.L. and E.B. contributed equally to this work.

Correspondence should be addressed to Netta Levin at [netta@hadassah.org.il](mailto:netta@hadassah.org.il).

<https://doi.org/10.1523/JNEUROSCI.3222-20.2021>

Copyright © 2021 the authors

## Introduction

*CNGA3*-achromatopsia is a congenital hereditary disease caused by cone-photoreceptor dysfunction, leading to impaired acuity, photoaversion, and color blindness (Wissinger et al., 2001). The majority of these patients have complete achromatopsia, with rod photoreceptor-driven vision only, essentially seeing the world in blurry shades of gray. A minority may manifest incomplete achromatopsia, with some residual cone function (Zelinger et al., 2015; Zobor et al., 2017). Using an ERG, photopic responses were nondetectable for complete *CNGA3*-ACHM but not for incomplete *CNGA3*-ACHM.

Following successful gene augmentation therapy in a naturally occurring ovine model (Banin et al., 2015; Gootwine et al., 2017), a phase I/IIa human trial was initiated in our center as

well as in other centers in the United States (ClinicalTrials.gov ID NCT02935517). In this trial, patients are treated with a single subretinal injection of an AAV2tYF capsid variant carrying the CNGA3 transgene under control of the engineered PR1.7 cone-specific opsin promoter in their worse eye. Additional gene augmentation trials for CNGA3 achromatopsia are being performed by two other groups (ClinicalTrials.gov IDs NCT02610582 and NCT03758404).

Restoration of visual function in adulthood has been of great interest in recent years. However, even if function recovers at the sensory organ level (eye/retina/optic nerve), it is questionable whether the visual cortex, deprived of input during critical developmental stages, will be able to extract and interpret relevant visual signals.

Leber congenital amaurosis is a severe congenital form of progressive retinal degeneration. One of the variants of this disease that is associated with mutations in the *RPE65* gene became the first Food and Drug Administration-approved gene augmentation treatment in humans (Russell et al., 2017). fMRI studies performed in patients undergoing this treatment showed increased response of the visual cortex to a flickering stimulus, demonstrating the preservation of light sensitivity after years of restricted vision (Cideciyan et al., 2014; Ashtari et al., 2017). However, behavioral studies suggest that congenitally visually deprived subjects still face severe visual difficulties even following restoration (Fine et al., 2003; Ostrovsky et al., 2006; McKyton et al., 2015). Cumulative evidence showing that adjacent and trans-synaptic wiring as well as the visual cortex itself can be affected by reduced input may provide a possible explanation (Baseler et al., 2002; Pascual-Leone et al., 2005). Furthermore, previously suggested reorganization of the deafferented visual cortex resulting from the influx of nonvisual information can interfere with processing the new visual input (Burton et al., 2002; Amedi et al., 2003).

The uniqueness of achromatopsia, in which cone-photoreceptors and afferent fibers are preserved but do not function, the therapeutic breakthrough of gene therapy for this disease, and the fact that the congenital lack of input affects cortical visual area development make it an attractive model to study cortical plasticity.

We herein report on two adult achromatopsia patients who underwent gene augmentation therapy. We report their visual function using standard and novel metrics, as well as their cortical activity using neuroimaging techniques. To the best of our knowledge, this is the first study to demonstrate cortical function both before and after restoring a congenital visual deficit.

## Materials and Methods

### Participants

Following the signing of informed consent approved by the local internal review board committee and the Israeli Ministry of Health, three subjects manifesting genetically confirmed CNGA3 achromatopsia were recruited at the Hadassah Medical Center in Jerusalem, Israel, as a single-site study. These same subjects are enrolled in a multicenter trial studying gene augmentation therapy in this disease [ClinicalTrials.gov ID NCT02935517, sponsored by Applied Genetic Technologies Corporation (AGTC)]. To date, two achromatopsia patients (one female; ages, 27 and 30 years) completed fMRI evaluations pretreatment and post-treatment, and herein we present their data. Six control participants (two females; mean  $\pm$  SD age,  $33 \pm 11$  years) were enrolled to serve as a control group for the fMRI tests. The add-on fMRI study was approved by the Hadassah Medical Center Ethics Committee, and written informed consent was obtained from patients and control participants.

Patient 1 is a 30-year-old male who has a background of allergic rhinitis and mild asthma, and is a smoker, but is otherwise healthy. He

manifested poor visual acuity, absent color vision, and photoaversion since infancy. Molecular genetic testing revealed a homozygous 130\_151 22 bp duplication (p.Ala51fs\*15) in the CNGA3 gene as the cause of disease (Zelinger et al., 2015; patient MOL 177–4). On baseline ocular examination, refractive error and best-corrected visual acuity were as follows: Right eye (RE): plano/−2.00  $\times$  20,  $42.7 \pm 0.6$  ETDRS letters; Left eye (LE): plano/−2.00  $\times$  170,  $43.7 \pm 0.6$  ETDRS letters. Anterior and posterior segments were essentially within normal limits, with very mild retinal pigmented epithelium (RPE) changes in the foveae. Optical coherence tomography (OCT) imaging revealed a small hyporeflexive area in the outer retina under the fovea, with mild disturbance of the ellipsoid zone but with preservation of the outer nuclear (photoreceptor nuclei) layer. Full-field ERG (FFERG) testing performed according to The International Society for Clinical Electrophysiology of Vision standard at 28 years of age and again at 30 years of age (before treatment) showed scotopic rod responses that were mildly reduced compared with normal and nondetectable cone responses under photopic conditions. Surgery that included vitrectomy and subretinal injection of the viral vector was uneventful, and serial OCT imaging postoperatively showed absorption of the subretinal fluid within <48 h. On long-term follow-up, retinal structure was well preserved both within and outside the treated area through the last time point examined at 12 months postsurgery. On ancillary testing, FFERG recordings 1 year post-treatment remained similar to baseline, without measurable improvement in cone responses.

Patient 2 is a 27-year-old female, who is generally healthy. Her disease manifestations are similar to those described in patient 1. Molecular genetic testing revealed a homozygous c.1585G>A (p.V529M) missense mutation in the CNGA3 gene as the cause of disease (Zelinger et al., 2015; patient MOL 1480–1). On baseline ocular examination, refractive error and best-corrected visual acuity were as follows: RE: +1/00/−0.75  $\times$  160,  $44.3 \pm 1.7$  ETDRS letters; LE: +1/00/−0.75  $\times$  10,  $40.3 \pm 1.5$  ETDRS letters. As in patient 1, examination of the anterior and posterior segments of the eyes was within normal limits, with very mild RPE changes in the foveae. On OCT imaging, mild disturbance of the ellipsoid zone was seen in the fovea with a small hyporeflexive area, while the photoreceptor nuclei layer was essentially preserved. Full-field ERG testing performed at baseline showed scotopic rod responses that were within normal limits, but cone responses under photopic conditions were nondetectable, as is often the case in achromatopsia. As in patient 1, serial OCT imaging showed that retinal structure remained well preserved through 4 months postsurgery, and FFERG results remained similar to those at baseline. It is important to note that this attests to the safety of the treatment.

### Procedure

The subjects were treated in one eye (the weaker eye) with AGTC-402, which is a nonreplicating, rep/cap-deleted, recombinant adeno-associated virus vector that expresses a codon-optimized human CNGA3 gene under control of the engineered PR1.7 cone opsin promoter (rAAV2tYF-PR1.7-hCNGAco; Gootwine et al., 2017). A volume of  $\sim$ 300 ml of viral suspension was injected into the subretinal space in the area of the posterior pole and macula following a standard three-port pars plana vitrectomy. Patient 1 was enrolled in cohort 2, and patient 2 was enrolled in cohort 4. The subjects were treated with perioperative systemic and topical steroids, which were tapered within 10 weeks postsurgery. In both subjects, the subretinal fluid resorbed within 48 h postsurgery with recovery of retinal structure, and the site of retinal penetration by the injection cannula healed well as demonstrated by serial OCT imaging.

### Assessment of visual function

Visual function tests and questionnaires were repeated three times at baseline and then administered at 1, 2, 3, 6, 9, and 12 months postsurgery. For analysis purposes, presurgery results were averaged to serve as a benchmark.

Questionnaires included the validated VFQ-39 (Mangione et al., 2001; National Eye Institute Visual Function Questionnaire; 25 questions + optional items, as described in the VFQ-25 manual), the VLSQ-8 (Verriotto et al., 2017; Visual Light Sensitivity Questionnaire; 8

questions), and an additional question concerning patient function under sunlight conditions (Table 1).

Best-corrected visual acuity was measured monocularly at 100% contrast using ETDRS charts (R, 1 and 2, in a certified lane; Precision Vision). We recorded the number of letters the patients reported correctly and used this number for analysis.

Color vision was separately measured in each eye using the Farnsworth-Munsell Dichotomous D-15 Test (X-Rite). The test was repeated twice at each visit. The total color difference score (TCDS) was used for analysis (Bowman, 1982; Table 2).

As an additional measure of color perception, a custom-made program to measure perceived color brightness was developed using Experiment Builder software (SR Research). Participants viewed a gray disk on a red background and were asked to change the brightness of the disk (by pressing the arrow keys) until the disk brightness best matched the background. The test was performed monocularly. This test was developed after both patients were treated and was administered once for each patient (at 12 and 4 months postsurgery for patients 1 and 2, respectively).

The degree of photoaversion was measured separately in each eye, as well as with both eyes open, using two types of light discomfort tests. In both tests, the subject is exposed to increasing intensities of light and reports (by pressing buttons) when an intensity that causes discomfort is reached. The first light discomfort test was performed using a newly developed photoaversion measurement device, the Ocular Photosensitivity Analyzer (OPA), which determines visual photosensitivity threshold via exposure to a two-dimensional (flat array) of LEDs (Verriotto et al., 2017). The test was performed while participants fixated on a fixation dot while their eye position was being monitored and captured. The OPA is considered to be more reliable than the second light discomfort test, which is performed using a Color Dome Ganzfeld device (Diagnosys), the same machine used for performing full-field ERG testing (Verriotto et al., 2017). This second test follows that described in the study by Adams et al. (2006), except that the stimulus is a full-field light and the test is performed with a mesopic background light. Briefly, eyes to be tested are adapted to a 3.0 cd/m<sup>2</sup> white (6500 K) background for 5 min before testing, and then the test is run in three studies per eye with 1 min between studies. The first stimulus is 0.6 log cd/m<sup>2</sup> (4 cd/m<sup>2</sup>), and each step increases in luminance by 0.3 log. Originally, 12 total steps were included, with the final step being 3.6 log cd/m<sup>2</sup> (3981 cd/m<sup>2</sup>), but, since some patients were able to reach higher intensities post-treatment, the following two additional steps were included: 3.78 log cd/m<sup>2</sup> (5775 cd/m<sup>2</sup>) and 3.9 log cd/m<sup>2</sup> (8000 cd/m<sup>2</sup>). Photoaversion assessment results using the two tests are detailed in Table 2.

#### Eye tracking

We took advantage of the fact that the OPA machine records a video of the participants' eyes to determine how well they can fixate before and after treatment. The participants placed their head on a chin and head rest, and fixated on a target while a camera, using infrared illumination, captured their eyes at 60 frames/s. The recording from the first few minutes was used for analysis up until the point in which participants started to move their head because of photoaversion (since during the test the patients are exposed to increasing intensities of light). To compare pretreatment and post-treatment recording sequences, the shortest sequence duration was chosen and used for both tests in each patient (200 s for patient 1 and 164 s for patient 2).

Using ImageJ software, we tracked the corneal reflection and pupil center of the eye. First, simple adjustment of brightness and contrast was performed to keep only the information of the pupil or the corneal reflection in the image. Then, TrackMate function was called to track either the pupil or the corneal reflection. The distance in pixels between the corneal reflection and the pupil center served as the eye position measure. To reduce noise resulting from blinks, samples 2 SDs above or below the average were excluded. Since we did not performed calibration, we cannot convert eye location unit from pixels to degrees. However, since all parameters were fixed between tests (head location/

**Table 1. Results of vision health status (VFQ-39) and sensitivity to light (VLSQ8) questionnaires**

	Patient 1		Patient 2	
	Pretreatment	Post-treatment	Pretreatment	Post-treatment
<b>A VFQ-39</b>				
General health	85, 100, 90	95	100, 100	88
General vision	75, 80, 55	<b>95</b>	55, 65	60
Ocular pain	75, 75, 63	<b>88</b>	100, 88	88
Near activity	63, 71, 54	<b>85</b>	88, 83	79
Distance activity	63, 88, 50	<b>94</b>	79, 83	75
Social functioning	100, 100, 83	100	100, 100	100
Mental health	60, 90, 70	80	50, 50	50
Role difficulties	56, 81, 50	<b>100</b>	31, 69	<b>75</b>
Dependency	75, 88, 81	81	81, 63	69
Driving	0, 0, 0	0	0, 0	0
Color vision	75, 75, 50	<b>100</b>	75, 50	75
Peripheral vision	75, 75, 50	<b>100</b>	75, 75	100
<b>B VLSQ8</b>				
1 (sensitivity outdoor)	1, 1, 3	1	4, 5	<b>2</b>
2 (glare)	2*	1	4, 4	<b>2</b>
3 (sensitivity to flickering light)	2, 2, 3	<b>1</b>	1, 1	1
4 (sensitivity severity)	3, 1, 3	1	3, 3	<b>1</b>
5 (headache)	3, 1, 2	2	3, 2	<b>1</b>
6 (blurry vision)	3, 2, 3	<b>1</b>	1, 2	1
7 (reading, watching screen)	1, 2, 4	1	4, 4	<b>1</b>
8 (sunglasses indoor)	4, 3, 3	<b>1</b>	1, 3	1
<b>C Added question</b>				
9 (function under sunlight)	3, 2, 3	<b>1</b>	5, 4	4

VFQ-39, Results of the VFQ-39 questionnaire that provides self-reported vision-targeted health status. A score of a 100 suggests no difficulty; the lower the score, the worse the function. VLSQ8, Results of the VLSQ8 questionnaire designed to detect visual sensitivity to light, with the topic of the question mentioned in parentheses; a score of 1 suggests no difficulty, while a score of 5 suggests the highest difficulty level. Added question, "How difficult do you find recognizing objects or performing tasks under bright sunlight?," with scoring the same as for VLSQ8. "Pretreatment" column shows the results of pretreatment visits. Asterisk denotes a question that was answered only in one visit. "Post-treatment" column show post-treatment results of the last visit (patient 1, 12 months post-treatment; patient 2, 6 months post-treatment). Post-treatment results that show improvement beyond the range of pretreatment results are marked using a bold font.

lighting), this measure is sufficient to indicate a change in fixation abilities resulting from treatment.

Eye tracking demonstrated repetitive fluctuations around the averaged eye position (typically, recorded in nystagmus patients; Fig. 1E). Maxima and minima of these fluctuations were detected, and the amplitudes (the difference between adjacent maximum and minimum) and frequencies (one divided by the duration between two maxima or two minima) of the nystagmus were measured and compared via *t* tests between pretreatment and post-treatment data and between data from treated and untreated eyes (see Table 4).

#### Experimental design and statistical analysis

**fMRI stimulus presentation.** Stimuli were projected binocularly under photopic conditions in the scanner onto a mirror placed above subjects' heads from a 32 inch MRI-compatible LCD Monitor (NordicNeuroLab), which was placed at a 140 cm viewing distance.

In the population-receptive field (pRF) fMRI experiment, a 2° wide black (0.37 cd/m<sup>2</sup>) and white (180 cd/m<sup>2</sup>) checkerboard bar moving parallel to its orientation was presented on a gray background (38 cd/m<sup>2</sup>). The bar moved 1°/s and completed its movement after 16 steps. Overall, the stimulus covered 16° of visual angle. Each run was composed of eight repetitions of bar movement in eight different directions plus four 12 s breaks with no stimulus presented. An additional break in the beginning of the run was not used for analysis. The VISTADISP toolbox and Psychtoolbox4 were used to create the stimuli.

In the ventral stream localizer fMRI experiment, we used a modified version of fLoc functional localizer (Stigliani et al., 2015) showing images of faces, limbs, houses, and textures, as well as color images that were

**Table 2. Assessment of visual function**

Test (units)	Patient	Time since surgery	Trials	Treated eye	Untreated eye	Untreated–treated	
Color perception Farnsworth D15 (TCDS)	1	Preoperative	3 (X2)	335.7 ± 53.3	307.8 ± 48.6	−27.9 ± 74.3	
		1–3 months	3 (X2)	300.8 ± 30.7	324.3 ± 24	23.5 ± 37	
		6–12 months	3 (X2)	305.8 ± 31.6	324.1 ± 37.5	18.3 ± 32	
	2	Preoperative	3 (X2)	327.3 ± 25.4	343.5 ± 45.8	16.2 ± 55.3	
		1–3 months	3 (X2)	320.8 ± 44	326.6 ± 58.3	5.9 ± 95.7	
		9–12 months	2 (X2)	294.3 ± 15.6	363 ± 35.9	68.7 ± 34.1	
	Best corrected visual acuity ETDRS (correctly reported letters)	1	Preoperative	3 (X1)	42.7 ± 0.6	43.7 ± 0.6	−1 ± 1
			1–3 months	3 (X1)	40.7 ± 4	43.3 ± 0.6	−2.7 ± 4.6
			6–12 months	3 (X1)	44.3 ± 0.6	45 ± 1	−0.7 ± 1.2
2		Preoperative	3 (X1)	40.3 ± 1.5	44.3 ± 1.7	−4 ± 1.2	
		1–3 months	3 (X1)	43.3 ± 2.1	47 ± 1	−3.7 ± 2.1	
		9–12 months	2 (X1)	44 ± 2.8	45 ± 2.8	−1 ± 0	
Light discomfort Ganzfeld (cd/m <sup>2</sup> )		1	Preoperative	2 (X3)	1292 ± 648	1667 ± 943	0.8 ± 0.1
			1–3 months	3 (X3)	4000 ± 0 <sup>#</sup>	972 ± 603	5.1 ± 2.4
			6–12 months	3 (X3)	6667 ± 2309	2500 ± 1893	3.3 ± 1.5
	2	Preoperative	4 (X3)	3458 ± 629	2099 ± 1539	1.5 ± 0.7	
		1–3 months	3 (X3)	7333 ± 1155	5806 ± 2001	1.3 ± 0.3	
		9–12 months	2 (X3)	8000 ± 0	8000 ± 0	1 ± 0	
	Light discomfort OPA (cd/m <sup>2</sup> )	1	Preoperative	3 (X1) <sup>~</sup>	8.7 ± 1.5	20.1 ± 15.3	0.6 ± 0.3
			3–6 months	3 (X1)	5206.5 ± 4583.2	523.4 ± 655.9	18.1 ± 21.3
			6–12 months	3 (X1)	2785.5 ± 525.3	1340 ± 198.5	5.2 ± 2
2		Preoperative	3 (X1)	18 ± 7.6	20.1 ± 13.4	1 ± 0.2	
		1–3 months	3 (X1)	59.4 ± 25.9	49.9 ± 27.2	1.2 ± 0.2	
		9–12 months	2 (X1)	185.2 ± 1.5	177.6 ± 53.6	1.1 ± 0.3	

Results are averaged, and the SD is shown across visits: presurgery visits are averaged; visits at 1, 2, and 3 months postoperation are averaged; and visits at 6, 9, and 12 months postoperation are averaged. At times where there was more than one trial per visit, the average value was taken for analysis (see parentheses under “Trials” column).

<sup>#</sup>Post-treatment, patient 1 showed marked reduction in photophobia and could tolerate even the highest intensity originally programmed for light discomfort in the Ganzfeld device, manifesting a “ceiling effect” (4000 cd/m<sup>2</sup>). On subsequent tests, two additional higher-intensity steps were added, as detailed in Materials and Methods.

<sup>~</sup>Marks that a different protocol was used for this patient at this time point (enhanced instead of normal testing mode; Verriotto et al., 2017) using the OPA machine. The different protocol causes a decreased threshold, however, the use of the ratio between the eyes is still comparable.

produced by adding hue to the texture images using Adobe Photoshop software. All images had a maximum intensity of 180 cd/m<sup>2</sup>, a minimum intensity of 0.37 cd/m<sup>2</sup>, and an average intensity between 33 and 83 cd/m<sup>2</sup>. Each 292 s run was composed of 73 blocks of 4 s each. Each block presented eight images in 2 Hz from the same category. Thirteen blocks were of a blank screen, and the rest were divided equally among the different categories. An additional two blocks at the beginning of the run were not used for analysis. The Presentation software (Neurobehavioral Systems) was used to combine the different stimuli into a movie presentation.

**fMRI data acquisition.** Scans were performed using a 32-channel coil in a 3 T MAGNETOM Skyra scanner (Siemens Healthcare).

Anatomical data were obtained using an MPRAGE sequence (TR, 2300 ms; TE, 2.98 ms; flip angle, 9°; isotropic voxel size, 1 mm; 160 axial 256 × 256 mm slices). Functional data were obtained using an EPI sequence (for the pRF experiment: TR, 1000 ms; TE, 34.4 ms; flip angle, 62°; isotropic voxel size, 2.5 mm; 48 slices; for the ventral stream localizer: TR, 1000 ms; TE, 32 ms; flip angle, 62°; isotropic voxel size, 2.5 mm; 52 slices). Four runs of the pRF experiment and two runs of the ventral stream localizer experiment were administered in every visit. The MRI data collection was performed once before surgery and 4 months after surgery. Patient 1 also performed the tests 8 and 12 months postsurgery. Control participants performed the MRI tests once.

**fMRI data analysis.** Analysis was performed using BrainVoyager software (Brain Innovation). Functional scans were preprocessed by correcting slice scan time and 3D motion, and by filtering out temporal frequencies <2 cycles. Functional scans were aligned to the anatomic scans, after which, both anatomic and functional scans were realigned to match MNI coordinates. For visualization, inflated maps were created by delineating the gray and white matter of each participant’s MPRAGE scan.

**Statistical analysis.** Analysis was performed using BrainVoyager software (Brain Innovation). For the pRF experiment, pRF model time courses were calculated based on the stimulus sequence for locations

−8° to 8° and for sizes 0.2° to 7°. The population-receptive field estimation procedure was performed in volume space, assigning each voxel a value of *R* (goodness of fit to the model), pRF location values, and a pRF size value. Early visual cortex (V1, V2, and V3 combined) was defined using a brain atlas (Wang et al., 2015). pRF size and eccentricity values from voxels within early visual cortex fitting the pRF model with *R* > 0.34 were used for analysis. Binning was performed for voxels using the following eccentricities: 0.2–1°, 1–2°, 2–4°, 4–6°, and 6–7°. To compare pretreatment and post-treatment results, patients’ binning was performed post-treatment using the same voxels as in the pretreatment analysis. For the ventral stream localizer experiment, a general linear model was generated, explaining the fMRI signal using the different block categories (faces, limbs, houses, colors, textures, and blank intervals). Color-selective regions were defined by voxels showing higher signal [*p* < 0.05, false discovery rate (FDR) corrected] in the color blocks than in the texture blocks. Voxels showing higher signal (*p* < 0.05, FDR corrected) in the face blocks compared with the house blocks were defined as face-selective regions. Voxels showing an opposite response were defined as place-selective regions.

For visualization purposes, pRF volume maps with voxels of *R* > 0.3 were projected into inflated cortical maps. The same projection was used for the ventral stream localizer experiment using voxels with *p* < 0.05 (FDR corrected) for each statistical test (faces > houses, houses > faces, and colors > textures).

**fMRI monocular assessment.** More than a year post-treatment, we performed a similar fMRI assessment, this time monocularly, comparing the treated versus the untreated eye. Similar fMRI stimulus presentation, data acquisition, data analysis, and statistical analysis was performed.

## Results

Following treatment, validated patient-reported outcome questionnaires designed to assess vision health status and sensitivity to light (Table 1, VFQ-39 and VLSQ-8) as well as free text self-reports

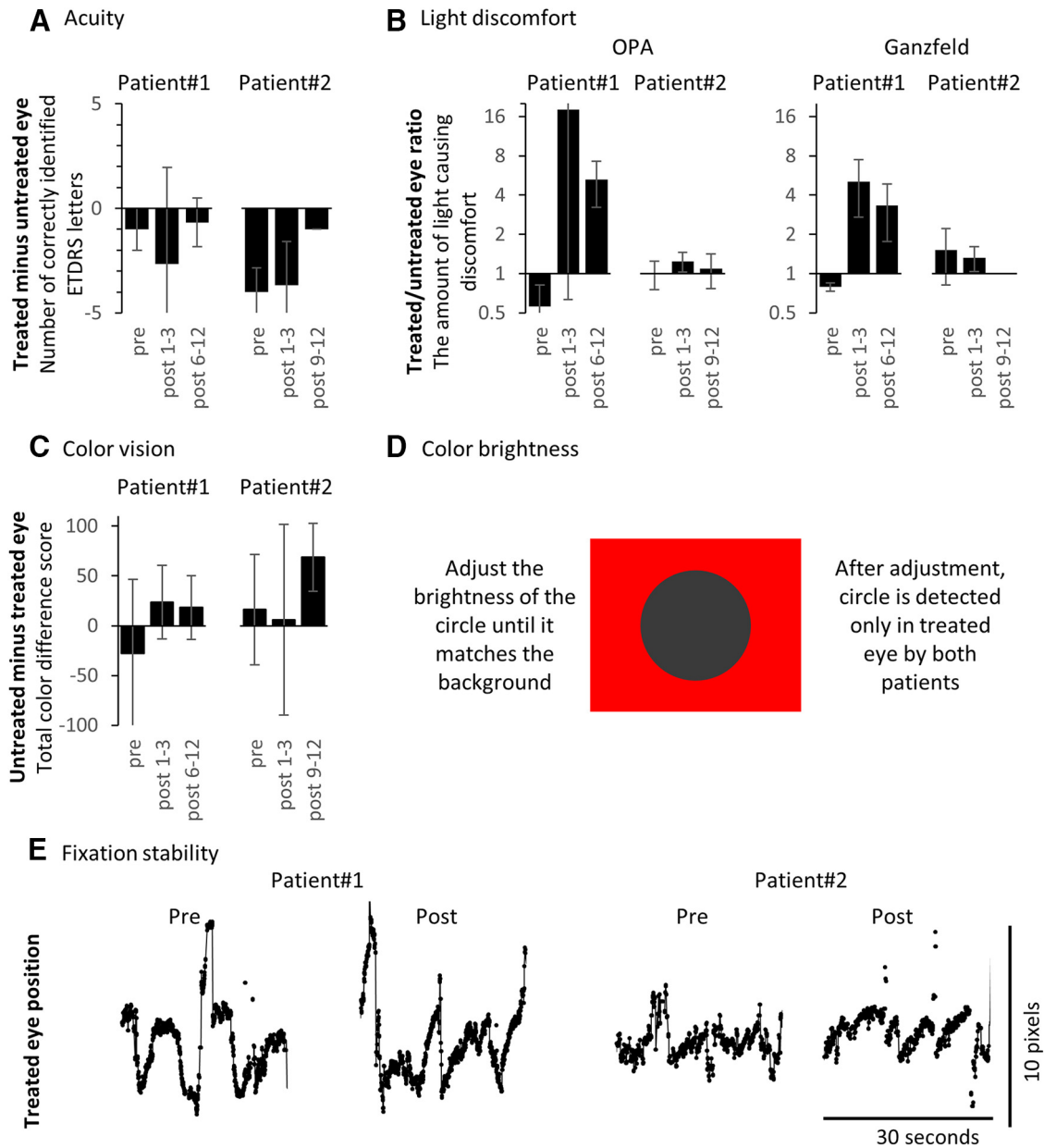


**Figure 1.** Visual function results. Comparison between treated and untreated eyes in different visual function tests. **A**, Number of correctly identified ETRDS letters in the treated minus the untreated eye. **B**, Ratio between the amount of light causing discomfort in the treated and untreated eyes, measured using the OPA and in the Color Dome Ganzfeld device. **C**, Farnsworth D-15 TCDS results in the treated minus the untreated eye. **D**, Color brightness test. After patients adjusted the brightness of the gray disk to mostly match the red background, detection of the disk was still apparent only in the treated eye (Table 2, numeric results). **E**, Eye-tracking measurements of the treated eye showing a sample of 30 s tracking before and after treatment while participants were asked to fixate. Since no calibration was performed, indication about eye position (the distance between corneal reflection and pupil center) was measured in pixels. In all bar charts, error bars represent standard deviation.

(Table 3), showed improvements in several measures of visual function. Formal testing of best-corrected visual acuity and photoaversion are shown in Table 2. A slight increase in acuity was evident in the treated eye of patient 2 (Fig. 1A). In addition, photoaversion decreased dramatically in the treated eye of patient 1 based on two separate light discomfort tests (Fig. 1B). In the OPA device, at baseline, the patient endured half the amount of light in the weaker eye (treated) compared with the stronger eye (untreated; mean  $\pm$  SD light intensity that causes discomfort in treated/untreated eye,  $0.56 \pm 0.25$ ). A year post-treatment, the treated eye could endure five times the intensity of the untreated eye ( $5.24 \pm 2.04$ ). There was no evidence of color perception improvement (Fig. 1C), although both patients reported “seeing red differently” after surgery. Because

rods are insensitive to longer wavelengths, achromats usually perceive red as almost black. Patients reported that post-treatment they started seeing red items even when they were presented on a black background (red light person icon on the pedestrian traffic light or red fixation light on the dark OPA device), items that they could not see pretreatment. Thus, a test designed to confirm their report was applied post-treatment. We reasoned that if there was cone function initiation, red, the only color rods are insensitive to, would be perceived differently in the treated eye compared with the untreated eye. Indeed, this was the case for both patients (Fig. 1D). When they were asked to change the brightness of a gray disk to match its red background, only the treated eye could detect the disk even when it was best matched by the patients. In the

**Table 3. Self-reporting by the patients during follow-up visits post-treatment**

Patients	
Patient 1	
2 months	Feels safer crossing the road as he can identify the vehicles approaching more easily (this continues to improve even 1 year post-treatment) Feels less photoaversion
3 months	Notices dust and smears on his glasses that he was oblivious to previously Feels he is able to better detect people entering his visual field
9 months	Better recognition of faces from a distance Feels he can better judge a person's age as wrinkles, facial features and skin changes are more apparent to him Sees red "differently" than before treatment in the treated eye
1 year	Switches on the light to find things on a shelf, whereas before treatment he would search in the dark No longer needs to use a magnifier to read forms with small print at work No longer needs to use sunglasses outside during daytime except on very sunny days Better vision at night which has been slowly improving since shortly after the treatment Can now recognize the bus number while the bus is still in motion before it arrives at the bus stop. Previously, prior to treatment, he needed the bus to be stationary in order to identify the number Improvement in self-confidence Improvement in fine motoric skills while using near vision (e.g., using fine tools to carve a straight line) During ski holiday felt much less photoaversion than during his ski holiday prior to treatment
Patient 2	
1 month	Manages to read documents easier and faster Was able to decrease font size on her smartphone
5 months	Reduction in photoaversion—can now walk outside during the daytime without having to wear sunglasses Notices that can now see when the red light in traffic lights is on. Prior to treatment could not identify this

untreated eye, a specific dark gray made the disk completely disappear for the patients.

Cortically, we first looked at the pRFs of voxels within the early visual cortex. We scanned participants while a flickering bar moved along their visual field. Using a model-driven approach, we estimated pRF eccentricities and sizes (Dumoulin and Wandell, 2008). Figure 2A presents eccentricity and size maps of the right hemisphere in a typical control and in the patients before and after surgery. The most striking difference was the large magnitude of the patients' pRF sizes (Fig. 2B), far beyond the range of typical cone-driven responses (Dumoulin and Wandell, 2008). Four months post-treatment, significant reductions in pRF sizes were observed in both patients, mostly in foveal regions. Patient 1 was also tested 8 and 12 months post-treatment, demonstrating no additional improvement.

To make sure that the differences we observed were driven by the treated eye, we rescanned the patients post-treatment (1.5 years post-treatment for patient 1; 1 year post-treatment for patient 2) also monocularly, comparing the treated to the untreated eye. As shown in Figure 2D, both patients exhibited smaller pRF sizes in the foveal regions of the treated eye.

To rule out the possibility that a change in the patients' fixation abilities served as a confounding factor for the reduction of the pRF sizes, we investigated eye movement patterns of the patients before and after treatment. Figure 1E shows 30 s samples of participants' eye tracking demonstrating their nystagmus pattern. Amplitudes and frequencies of the nystagmus were measured and compared between pretreatment and post-treatment data and between data from treated and untreated eyes, showing no difference in eye movement pattern (Table 4).

The second fMRI experiment was designed to explore ventral stream visual areas. To that end, a block design experiment was used, presenting blocks of houses, faces, and grayscale/colored textures. In all controls, typical ventral stream organization was demonstrated (Fig. 3A). As expected (Lafer-Sousa et al., 2016), a color-sensitive region was located between a medial place region and a lateral face region (Fig. 2C). Both patients showed a similar pattern of activation for faces and houses, suggesting achromatopsia does not prevent typical development of color-nonspecific high-ventral stream regions. This might not be surprising since patients'

vision, even before treatment, allow them to recognize people and navigate independently in everyday life. However, in these participants, not even one voxel showed specificity to color, before or after treatment. Similar results were evident in the follow-up monocular fMRI assessment, demonstrating no color-specific voxels regardless of the eye tested.

## Discussion

Following gene therapy-mediated visual restoration treatment in two achromatopsia patients, receptive field sizes of early visual areas decreased in the treated eye, suggesting better resolution. This is in accordance with patients' description of better detailed everyday vision and with the trend of improvement we found in the acuity measurements in patient 2, which is of a magnitude similar to that reported by Fischer et al. (2020). On the other hand, these patients showed no evidence for cortical color-specific regions. This cortical deficit is in accordance with the absence of color perception in a standardized test (although red detection was observed) and with Fischer et al. (2020), who found marginal improvement 6 months postsurgery that was abolished 6 months later. The absence of color perception and color-sensitive voxels, even at 1 year postsurgery (Fig. 3B), might stem from insufficient activation of cone photoreceptors at the retinal level, thus not providing adequate input, or, if cones were indeed activated, from a lack of ability to process that input.

It is important to note that our assumption is that at the retinal level cones were indeed activated following the gene augmentation treatment. The fact that full-field ERG cone-derived responses remained nondetectable following treatment does not support this assumption, but does not rule it out either. The area of the retina that was treated is relatively small, and thus the response in all probability would still be below that which can be detected by the external ERG electrodes that are placed on the surface of the eye. In fact, in patients with retinitis pigmentosa that manifest widespread retinal degeneration, it is not rare to find that ERG responses are nondetectable under all stimulus conditions while good central visual acuity and measurable visual fields that are cone mediated are still present. We believe that both our behavioral

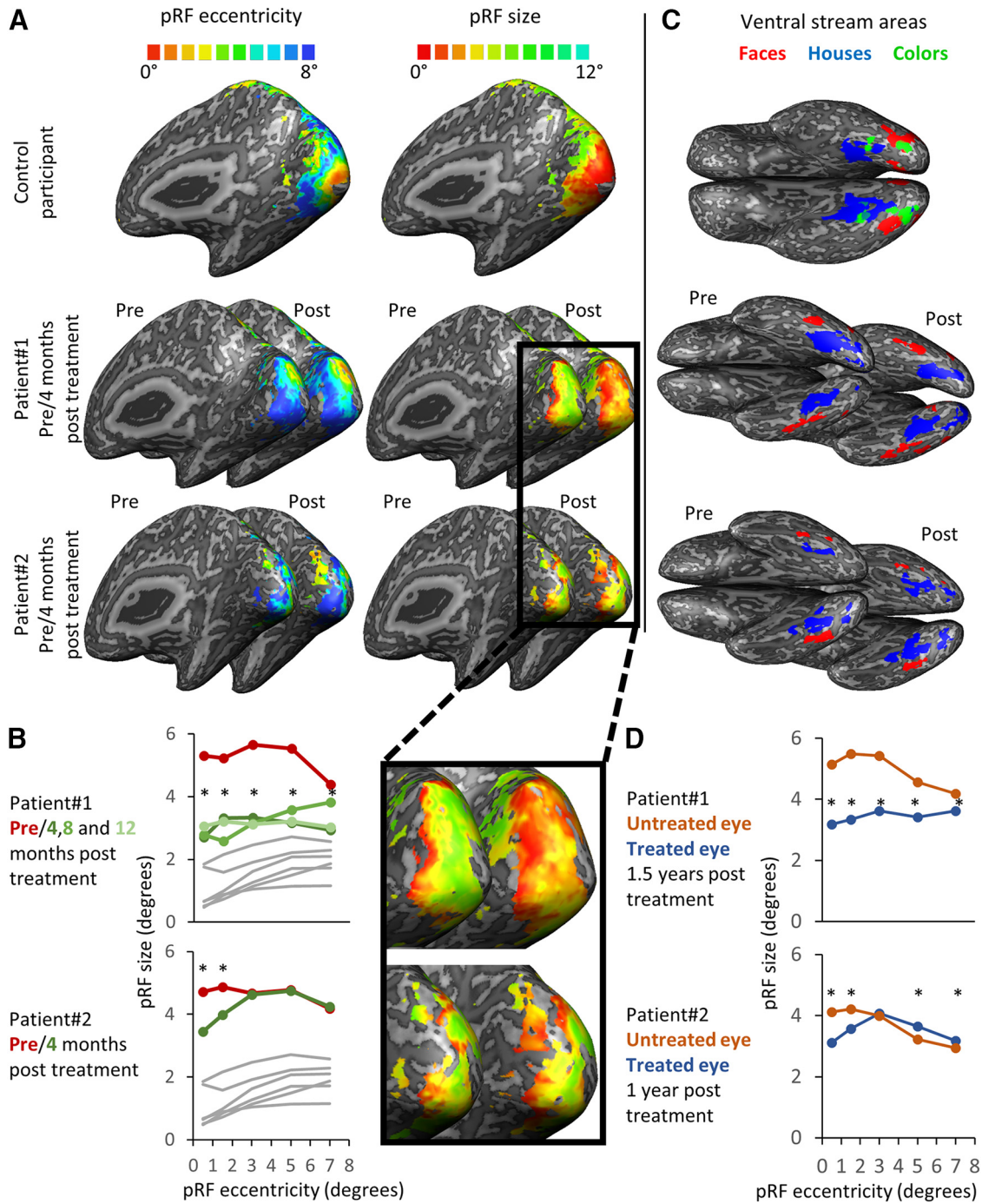


**Figure 2.** fMRI results. **A**, Participants’ pRF eccentricity (left) and size (right) maps drawn on individual inflated maps of the right hemisphere. **B**, Patients’ pRF sizes in each eccentricity bin (0.2–1°, 1–2°, 2–4°, 4–6°, 6–7°) within early visual cortex voxels exceeding  $R = 0.34$ , before and after treatment. Gray curves denote control data. Asterisks denote a significant difference in pRF size across voxels in a specific bin exceeding  $R = 34$  ( $p < 0.0001$ , Bonferroni-corrected) between presurgery and 4 months after surgery. **C**, Participants’ inflated cortical maps showing faces (red), places (blue), and color (green) regions. **D**, Same as **B** except that stimuli were presented in a monocular fashion post-treatment, comparing pRF sizes of the treated and untreated eyes. Note the similarity to the pretreatment and post-treatment graphs in **B**.

and cortical findings, especially our monocular results, support the assumption that some restoration of cone function did occur following treatment. Behaviorally, only the operated eye detected a red color. Cortically, pRF sizes were smaller specifically in the fovea of the treated eye, the treated area that exhibits high cone density. The reduction in the size of receptive fields could be driven directly from activity initiation of cones but also from diverse rod–cone interactions causing the signals to mix at virtually every level of signal processing (Fain and Sampath, 2018). Interestingly, it was recently

reported that in primates activating either type of photoreceptor briefly suppresses the responses of the other (Grimes et al., 2015).

It is important to note that patients’ reports regarding color perception, though very consistent, were subtle. They reported seeing only red and only on a very dark background in the treated eye while not being able to observe this in the untreated eye. We can suggest the following two explanations for this subtle effect: the first is that only L-cone function recovered, and when now coupled with rod activity that mediates vision in achromatopsia patients also

**Table 4. Eye-tracking statistical analysis results**

		Treated eye		Untreated eye		$p$ Value treated/untreated	
Patient 1	Pre	Amplitude (pixels)	3.70	$\pm 2.15$	3.32	$\pm 1.87$	0.37
		Frequency (1/s)	0.17	$\pm 0.14$	0.25	$\pm 0.28$	0.11
	Post	Amplitude (pixels)	3.49	$\pm 2.33$	4.00	$\pm 1.99$	0.23
		Frequency (1/s)	0.29	$\pm 0.39$	0.29	$\pm 0.29$	0.96
	$p$ value pre/post	Amplitude	0.66		0.07		
	Frequency	0.07		0.46			
Patient 2	Pre	Amplitude (pixels)	2.40	$\pm 1.17$	2.39	$\pm 1.08$	0.69
		Frequency (1/s)	0.19	$\pm 0.12$	0.19	$\pm 0.09$	0.90
	Post	Amplitude (pixels)	1.99	$\pm 0.87$	1.92	$\pm 1.14$	0.80
		Frequency (1/s)	0.34	$\pm 0.49$	0.37	$\pm 0.61$	0.83
	$p$ value pre/post	amplitude	0.14		0.11		
	frequency	0.13		0.13			

Eye-tracking sequences showed nystagmus. An amplitude was defined as the difference between adjacent maximum and minimum, and the frequency was defined as 1 divided by the duration between two maxima or two minima. The table shows the mean and SD of the amplitude and frequency of the eye movement pattern in each eye, pretreatment (pre) and post-treatment (post) and in each patient.  $p$  Values of  $t$  tests that were performed between data for treated and untreated eyes, and between pretreatment and post-treatment data are presented as well.

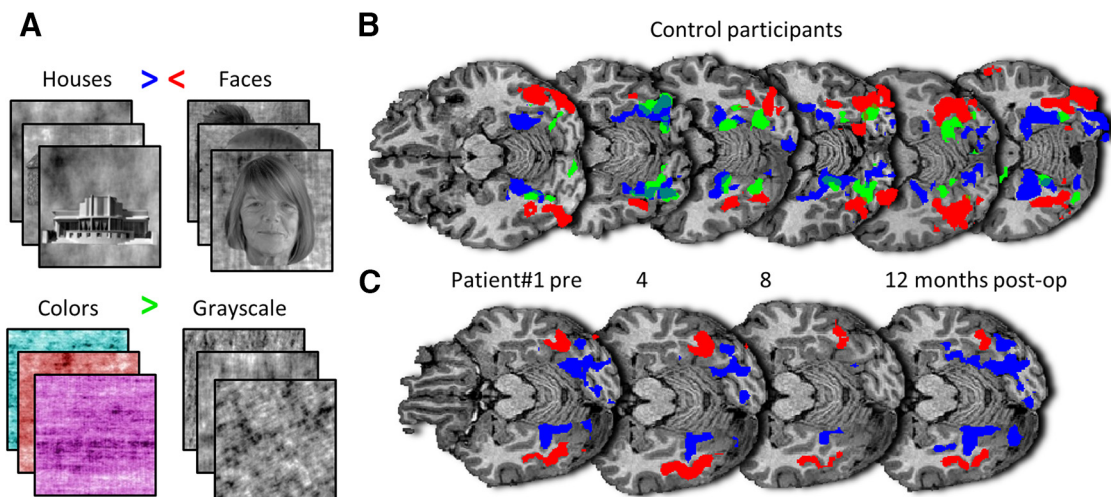


**Figure 3.** Ventral stream localizer results. **A**, Stimuli used to define faces (red), places (blue), and color (green) regions. Colored “greater-than” and “less-than” symbols denote the contrasts used for regions definition (i.e., blue voxels show a higher response to houses than faces images). **B**, **C**, Localizer results for all six control participants and in all visits for patient 1 showing visual-specific regions for faces (red), places (blue), and color (green).  $p < 0.05$ , FDR corrected.

under photopic conditions (Zelinger et al., 2015), a limited ability to detect red color emerges. This hypothesis is based on previous studies showing that people with only one type of cones (S-cone monochromats) can use cone activity together with the rod input to perceive color in a limited part of the spectrum (Reitner et al., 1991). The second possibility is that, similar to primates treated with the same promotor (Ye et al., 2016), all cone types recovered. In this case, the reason for the limited color perception could be driven by hyperactivity of the rods. We only see behavioral evidence for the activity of L-cones since the M-cones and S-cones overlap with the spectrum of rods.

Additionally, the lack of more pronounced recovery of color vision at the behavioral level and the lack of evidence for activity of cortical color-specific regions on fMRI may reflect a failure to process and encode the input at the cortical level. The question of whether providing “visual input” results in “restoring sight” has accompanied innovative vision restoration attempts since they began. It is known that cortical plasticity differs along visual brain hierarchy and different stages of life (Beyeler et al., 2017). Thus, our study is unique in three aspects. First, restoration was applied in adulthood for a congenital impairment. Similar to delayed cochlear implantation, which markedly decreases speech understanding (Kral and O’Donoghue, 2010), it is reasonable to

assume that deafferented color areas did not develop in congenital achromatopsia patients and therefore color perception might not accompany cone function restoration. Second, the impairment affects both early and high-order visual areas. Previous behavioral studies in late emergence from congenital blindness suggest that shape recognition following low-level cues is regained, while mid-level-based vision remains deficient (McKyton et al., 2015). This can be explained further by the presence of retinotopic organization in early visual areas in early blind individuals (Bock et al., 2015). Finally, our study attempts to link behavior and cortical data. To the best of our knowledge, the only case reported in the literature describing functional cortical differences along the visual hierarchy following prolonged visual deprivation and restoration is the case of MM, who was blinded at the 3 years of age, regained vision at 46 years of age, and was tested years later (Fine et al., 2003; Levin et al., 2010). As in our cases, the pRF sizes of MM’s estimated early near-foveal visual areas were larger than those of controls and high-level visual functional areas were absent. These fMRI results were in accordance with MM’s limited visual abilities despite regained retinal function.

To conclude, both patients report seeing only slightly better. One patient who has less sensitivity to light, removed his sunglasses

and showed reduction in photophobia. The other patient decreased the font size on her phone and showed marginal improvement in the acuity test. Generally speaking, differences in treatment outcomes between the patients in this trial can stem from multiple factors. These include factors related to delivery of the medication, such as differences in the concentration of the viral vector (as part of the multicenter dose escalation protocol, each of the patients received a different viral concentration), the volume of fluid that was delivered into the subretinal space, and the location and extent of the area treated, the degree of reflux, and the rate of absorption of the subretinal fluid. A second set of factors are patient-specific factors such as possibly differing immune responses, differences in efficacy of transfection and levels of expression, variable cone-rod interactions within the retina, and others. However, the unifying and encouraging aspect is the reduction in the pRF sizes post-treatment. These results were consistent in both the monocular and binocular fMRI studies, thus stressing that the brain can still code a new input at adulthood, at least to a limited degree, and higher doses, vision training, and longer follow-up duration could potentially allow additional improvements in function. An additional consideration is the age of treatment. It is quite plausible to think that complete achromatopsia patients may be deeply amblyopic to cone input, which they essentially had not been exposed to since birth. If this is the case, the perception of high-order functions such as color vision may be difficult to attain if reactivation of cone function at the retinal level is performed at ages beyond the amblyopia treatment window. Earlier intervention may be beneficial to avoid such “cone-amblyopia” and may help to optimize patient outcomes.

## References

- Adams WH, Digre KB, Patel BCK, Anderson RL, Warner JEA, Katz BJ (2006) The evaluation of light sensitivity in benign essential blepharospasm. *Am J Ophthalmol* 142:82–87.
- Amedi A, Raz N, Pianka P, Malach R, Zohary E (2003) Early “visual” cortex activation correlates with superior verbal memory performance in the blind. *Nat Neurosci* 6:758–766.
- Ashtari M, Nikonova ES, Marshall KA, Young GJ, Aravand P, Pan W, Ying GS, Willett AE, Mahmoudian M, Maguire AM, Bennett J (2017) The role of the human visual cortex in assessment of the long-term durability of retinal gene therapy in follow-on RPE65 clinical trial patients. *Ophthalmology* 124:873–883.
- Banin E, Gootwine E, Obolensky A, Ezra-Elia R, Ejzenberg A, Zelinger L, Honig H, Rosov A, Yamin E, Sharon D, Averbukh E, Hauswirth WW, Ofri R (2015) Gene augmentation therapy restores retinal function and visual behavior in a sheep model of *CNGA3* achromatopsia. *Mol Ther* 23:1423–1433.
- Baseler HA, Brewer AA, Sharpe LT, Morland AB, Jägle H, Wandell BA (2002) Reorganization of human cortical maps caused by inherited photoreceptor abnormalities. *Nat Neurosci* 5:364–370.
- Beyeler M, Rokem A, Boynton GM, Fine I (2017) Learning to see again: biological constraints on plasticity. *J Neural Eng* 14:051003.
- Bock AS, Binda P, Benson NC, Bridge H, Watkins KE, Fine I (2015) Resting-state retinotopic organization in the absence of retinal input and visual experience. *J Neurosci* 35:12366–12382.
- Bowman KJ (1982) A method for quantitative scoring of the Farnsworth panel D-15. *Acta Ophthalmol (Copenh)* 60:907–916.
- Burton H, Snyder AZ, Diamond JB, Raichle ME (2002) Adaptive changes in early and late blind: a fMRI study of verb generation to heard nouns. *J Neurophysiol* 88:3359–3371.
- Cideciyan AV, Aguirre GK, Jacobson SG, Butt OH, Schwartz SB, Swider M, Roman AJ, Sadigh S, Hauswirth WW (2014) Pseudo-fovea formation after gene therapy for RPE65-LCA. *Invest Ophthalmol Vis Sci* 56:526–537.
- Dumoulin SO, Wandell BA (2008) Population receptive field estimates in human visual cortex. *Neuroimage* 39:647–660.
- Fain G, Sampath AP (2018) Rod and cone interactions in the retina. *F1000Res* 7:657.
- Fine I, Wade AR, Brewer AA, May MG, Goodman DF, Boynton GM, Wandell BA, MacLeod DIA (2003) Long-term deprivation affects visual perception and cortex. *Nat Neurosci* 6:915–916.
- Fischer MD, Michalakis S, Wilhelm B, Zobor D, Muehlfriedel R, Kohl S, Weisschuh N, Ochakovski GA, Klein R, Schoen C, Sothilingam V, Garcia-Garrido M, Kuehlewein L, Kahle N, Werner A, Dauletbekov D, Paquet-Durand F, Tsang S, Martus P, Peters T, et al (2020) Safety and vision outcomes of subretinal gene therapy targeting cone photoreceptors in achromatopsia: a nonrandomized controlled trial. *JAMA Ophthalmol* 138:643–651.
- Gootwine E, Ofri R, Banin E, Obolensky A, Averbukh E, Ezra-Elia R, Ross M, Honig H, Rosov A, Yamin E, Ye GJ, Knop DR, Robinson PM, Chulay JD, Shearman MS (2017) Safety and efficacy evaluation of rAAV2YF-PR1.7-hCNGA3 vector delivered by subretinal injection in *CNGA3* mutant achromatopsia sheep. *Hum Gene Ther Clin Dev* 28:96–107.
- Grimes WN, Graves LR, Summers MT, Rieke F (2015) A simple retinal mechanism contributes to perceptual interactions between rod- and cone-mediated responses in primates. *Elife* 4:e08033.
- Kral A, O’Donoghue GM (2010) Profound deafness in childhood. *N Engl J Med* 363:1438–1450.
- Lafer-Sousa R, Conway BR, Kanwisher NG (2016) Color-biased regions of the ventral visual pathway lie between face- and place-selective regions in humans, as in macaques. *J Neurosci* 36:1682–1697.
- Levin N, Dumoulin SO, Winawer J, Dougherty RF, Wandell BA (2010) Cortical maps and white matter tracts following long period of visual deprivation and retinal image restoration. *Neuron* 65:21–31.
- Mangione CM, Lee PP, Gutierrez PR, Spritzer K, Berry S, Hays RD (2001) Development of the 25-item National Eye Institute visual function questionnaire. *Arch Ophthalmol* 119:1050–1058.
- McKyton A, Ben-Zion I, Doron R, Zohary E (2015) The limits of shape recognition following late emergence from blindness. *Curr Biol* 25:2373–2378.
- Ostrovsky Y, Andalman A, Sinha P (2006) Vision following extended congenital blindness. *Psychol Sci* 17:1009–1014.
- Pascual-Leone A, Amedi A, Fregni F, Merabet LB (2005) The plastic human brain cortex. *Annu Rev Neurosci* 28:377–401.
- Reitner A, Sharpe LT, Zrenner E (1991) Is colour vision possible with only rods and blue-sensitive cones? *Nature* 352:798–800.
- Russell S, Bennett J, Wellman JA, Chung DC, Yu Z-F, Tillman A, Wittes J, Pappas J, Elci O, McCague S, Cross D, Marshall KA, Walshire J, Kehoe TL, Reichert H, Davis M, Raffini L, George LA, Hudson FP, Dingfield L, et al (2017) Efficacy and safety of voretigene neparovec (AAV2-hRPE65v2) in patients with RPE65-mediated inherited retinal dystrophy: a randomised, controlled, open-label, phase 3 trial. *Lancet* 390:849–860.
- Stigliani A, Weiner KS, Grill-Spector K (2015) Temporal processing capacity in high-level visual cortex is domain specific. *J Neurosci* 35:12412–12424.
- Verriotto JD, Gonzalez A, Aguilar MC, Parel J-MA, Feuer WJ, Smith AR, Lam BL (2017) New methods for quantification of visual photosensitivity threshold and symptoms. *Transl Vis Sci Technol* 6:18.
- Wang L, Mruczek REB, Arcaro MJ, Kastner S (2015) Probabilistic maps of visual topography in human cortex. *Cereb Cortex* 25:3911–3931.
- Wissing B, Gamer D, Jägle H, Giorda R, Marx T, Mayer S, Tippmann S, Broghammer M, Jurkies B, Rosenberg T, Jacobson SG, Sener EC, Tatlipinar S, Hoyng CB, Castellani C, Bitoun P, Andreasson S, Rudolph G, Kellner U, Lorenz B, et al. (2001) *CNGA3* mutations in hereditary cone photoreceptor disorders. *Am J Hum Genet* 69:722–737.
- Ye GJ, Budzynski E, Sonnentag P, Nork TM, Sheibani N, Gurel Z, Boye SL, Peterson JJ, Boye SE, Hauswirth WW, Chulay JD (2016) Cone-specific promoters for gene therapy of achromatopsia and other retinal diseases. *Hum Gene Ther* 27:72–82.
- Zelinger L, Cideciyan AV, Kohl S, Schwartz SB, Rosenmann A, Eli D, Sumaroka A, Roman AJ, Luo X, Brown C, Rosin B, Blumenfeld A, Wissing B, Jacobson SG, Banin E, Sharon D (2015) Genetics and disease expression in the *CNGA3* form of achromatopsia: steps on the path to gene therapy. *Ophthalmology* 122:997–1007.
- Zobor D, Werner A, Stanzial F, Benedicenti F, Rudolph G, Kellner U, Hamel C, Andréasson S, Zobor G, Strasser T, Wissing B, Kohl S, Zrenner E (2017) The clinical phenotype of *CNGA3*-related achromatopsia: pre-treatment characterization in preparation of a gene replacement therapy trial. *Invest Ophthalmol Vis Sci* 58:821–832.